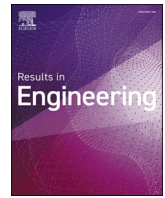




Contents lists available at ScienceDirect

Results in Engineering

journal homepage: www.sciencedirect.com/journal/results-in-engineering

Waste-based panels with cement grout as an infill material for composite railway sleepers

Mamun Abdullah^a, Wahid Ferdous^{a,*}, Sourish Banerjee^a, Ali Mohammed^b, Allan Manalo^a

^a University of Southern Queensland, Centre for Future Materials (CFM), School of Engineering, QLD, 4350, Australia

^b Technical Lead, Wagners CFT, Wellcamp, QLD, 4350, Australia

ARTICLE INFO

Keywords:

Composite railway sleepers
Bond behaviour
Sleeper bending strength
Wood composites
Recycled plastics

ABSTRACT

The development of high performance and eco-friendly composite railway sleepers at a reasonable price is a great challenge for composite railway sleeper manufacturers. The study proposed a railway sleeper concept based on high-performance fibre composites and low-cost waste-based materials to overcome this challenge. In this concept, thin hollow composite tubes are filled with high volume waste-based panels, which are bonded together with cement grout. This study examined the effect of cement grout, grout thickness, panel types, and surface preparation of the panels on the bond behaviour between the panels and cement grout. It also investigated the bending behaviour of manufactured railway sleepers by evaluating the effects of filling hollow tubes, the orientation of the infill panels, and the types of infill materials. Results indicate that the proposed concept has a high potential for development of high performance and eco-friendly composite railway sleepers at a competitive price due to the incorporation of high volume of waste materials. The results of the study will serve as a guide to the manufacture and design of composite railway sleepers.

1. Introduction

Railway sleepers are traditionally made of timber, steel and concrete. There are several challenges facing these sleeper materials. The decaying, splitting, and insect-attacking characteristics of timber, as well as its scarcity, posed new challenges. The corrosive nature, high electrical conductivity, and fatigue cracking of steel sleepers in the rail-seat region, as well as the difficulty of packing with ballast, make steel sleepers a less preferred material for use in sleepers. Contrary to timber and steel, prestressed concrete sleepers are heavy, have a high initial cost, have limited impact resistance, and are susceptible to chemical attack [1]. Heavy weights result in higher transportation costs, are difficult to handle, and require costly, specialised equipment to be installed. Concrete and steel sleepers require specific fasteners and cannot be substituted for timber sleepers in an existing track due to their incompatibility [2]. Traditional sleeper materials create several environmental problems from a sustainable perspective; for example, countless trees must be cut down to produce timber sleepers, while the cement and steel industries release a large amount of carbon dioxide during production. In response to the issues, researchers around the world have developed and investigated alternative sleeper technologies.

The strength, lightweight characteristics, superior workmanship, and design versatility of composite materials make them ideal for use as structural components in a wide range of engineering applications [3–5]. Researchers have examined composites as an alternative to traditional materials for developing sustainable railway sleepers. Typically, composite railway sleepers are made from either fibre composites or recycled plastics [6,7]. Recently, the authors examined several concepts for composite railway sleepers, including design concepts with internal and external reinforcements [7–9]. These sleepers, however, were made of resin-based polymer concrete, which is relatively more expensive than traditional railway sleeper materials. Fibre composite sleepers, particularly fibre-reinforced foamed urethane (FFU) [10], are exceedingly costly (five to ten times more expensive than timber sleepers [11]), have low shear resistance due to the absence of transverse reinforcements, and have caused concern about compliance with Occupational Health, Safety, and Environment (OHSE) guidelines due to the generation of polyurethane dust during drilling [12]. Recycled plastic sleepers [13,14] can be manufactured at a comparable price to timber sleepers, but their low screw-holding capacity, low stiffness, crack formation due to low bending strength, high thermal expansion, poor dimensional stability at elevated in-service temperatures, plastic

* Corresponding author.

E-mail addresses: Mamun.AlMamun@unisq.edu.au (M. Abdullah), Wahid.Ferdous@unisq.edu.au (W. Ferdous), Sourish.Banerjee@unisq.edu.au (S. Banerjee), ali.mohammed@wagner.com.au (A. Mohammed), Allan.Manalo@unisq.edu.au (A. Manalo).

<https://doi.org/10.1016/j.rineng.2024.102924>

Received 29 June 2024; Received in revised form 8 September 2024; Accepted 16 September 2024

Available online 17 September 2024

2590-1230/© 2024 The Authors. Published by Elsevier B.V. This is an open access article under the CC BY license (<http://creativecommons.org/licenses/by/4.0/>).

deformation that loosens fasteners, low fire resistance, and lack of track-bed stability due to their low weight have limited their use [6,15]. It is therefore necessary to develop a composite railway sleeper that is cost-effective, environmentally friendly, and can meet performance criteria. Integration of waste-based materials with fibre composites is one strategy to achieve this goal. An example of such a concept is shown in Fig. 1.

The proposed concept uses a Glass Fibre Reinforced Polymer (GFRP) tube filled with waste-based panel materials and bonded with cement grout. It is expected that the GFRP tube will provide structural strength to the beam, infill waste panels will increase the sectional modulus, and cement grout will enable the beam to act as a composite unit. To understand the overall behaviour of railway sleepers, it is necessary to understand the proper design of cement grout and how it interacts with waste-based panels. Therefore, this study investigates the bonding behaviour between cement grout and panels, the orientation and type of infill panels, and the bending behaviour of railway sleepers. This study is expected to provide guidelines for designing and manufacturing of railway sleepers made from waste-based materials and fibre composites.

2. Materials and methods

2.1. Materials

This study utilised waste-based composite wood and recycled plastic panels, cement grout mixed with waste glass sand, and GFRP hollow composite tubes. Waste-based panels were placed in GFRP hollow tubes and bonded with cement grout to manufacture composite beams.

2.1.1. Waste-based panels

Railway sleepers are manufactured using two distinct segments of composite material, consisting of wood and recycled plastic (Fig. 2). This engineered wood product is manufactured by Coen Composite Woods, which replaces traditional wood with an environmentally friendly alternative. It is composed of 60 % recycled wood flour, 30 % recycled High-density polyethylene (HDPE) plastic, and 10 % bonding agent [16]. Replas, on the other hand, supplies recycled plastic panels consisting of 100 % recycled HDPE and Polypropylene (PP), which offer a viable alternative to timber, which is susceptible to termites and moisture damage [17]. The densities of wood composite and recycled plastic panels are 1300 kg/m³ and 900 kg/m³, respectively.

2.1.2. Cement grout

General purpose cement (GP cement) and water were mixed with or without waste glass sand to prepare cement grout. Water-cement ratios of 0.35, 0.40 and 0.45 were used to maintain a good balance between bond strength and workability. Cement grout blended with glass sand provides sustainability and improved material properties, making it a viable option for environmentally conscious and high-performance building applications.

2.1.3. Fibre composite tubes

In order to understand composite beam behaviour, Wagners Pty Ltd [18] supplied pultruded GFRP hollow tubes. The dimensions of the rectangular hollow section (RHS) of GFRP were 1.60 m long, 250 mm

wide, and 100 mm deep, with a wall thickness of 8.1 mm. Hollow rectangular profiles enhance structural efficiency while reducing material consumption, making them cost effective. Moreover, their non-conductive nature makes them ideal for applications requiring low electrical conductivity. The innovative GFRP sections redefine the possibilities in modern construction, providing solutions that contribute to the sustainability of infrastructure projects in addition to being durable and efficient. The properties of fibre composite tubes are presented in Table 1.

2.2. Design of experiments using Taguchi method

The multiple levels and variables involved in the process can make it both time-consuming and costly. In order to reduce the number of necessary experiments, the Taguchi method [19] maintains an understanding of the influence each variable has on the outcome. In this method, the best results are obtained when there are a moderate number of variables (3–50), minimal interactions between them, and only a few variables have significant influence on the entire process. In the Taguchi experimentation, the following steps should be followed: deciding the design parameters and determining the number of levels for each level; choosing the optimal orthogonal array and placing it based on the parameters and levels; conducting experiments based on this arrangement; and analysing the results using Analysis of Variance (ANOVA) and signal-to-noise ratios (SNR). Table 2 shows four variables and three levels considered in the study. The most important parameters influencing the behaviour of bonds were identified systematically. To fully understand bond behaviour, the traditional approach requires 81 experiments (i.e., 3⁴). By employing the Taguchi design of experiments, the number of experiments was reduced to nine without compromising understanding of each parameter.

2.2.1. Design parameters and levels selection

Different parameters influence bond strength, including grout properties, bond length, bond thickness, bond width, panel types, surface roughness, and curing temperature, method, and time. This study considers grout properties (water-to-cement ratio), bond thickness, panel type and surface coating, all of which have three levels, as shown in Table 2. Based on the results of a preliminary investigation [20], the levels for parameters A and B were determined, while for parameters C and D they were set based on the expected outcomes of the final application. A cement grout with a water-to-cement ratio of 0.35–0.45 is suitable for coating and binding panels. It has been reported by Ferdous et al. [20] that the effective bond thickness for FRP-to-polymer bonds is 5 mm. In a similar study, concrete and FRP were bonded with non-porous glue materials [21]. This type of bond produces a very thin bond (generally less than 1 mm), which is incompatible with cement grout as it contains a porous filler material. Further, glue laminated bonds are applied using a brush, whereas cement grout bonds require a wider gap between the adherents. Therefore, bond thicknesses of 3 mm–10 mm were considered reasonable. A consideration of sustainability and availability was made when choosing panel types. The findings of Abdullah et al. [22] indicated that the surface coatings have a significant impact on bond behaviour, and this has been taken into account when designing this study.

To calculate the number of experiments that will be required, orthogonal arrays are used (Table 3), which are the most compact matrix of combinations that involve simultaneous changes to all selected design parameters. An orthogonal array has a certain number of degrees of freedom (DOF) that represents the number of levels considered for each parameter. This quantity can be calculated using Eq. (1).

$$DOF = L - 1 \quad (1)$$

There must not be a lower degree of freedom (DOF) in the orthogonal array than in the total degree of freedom (DOF). The four design parameters, A, B, C, and D, each had three levels with two degrees of

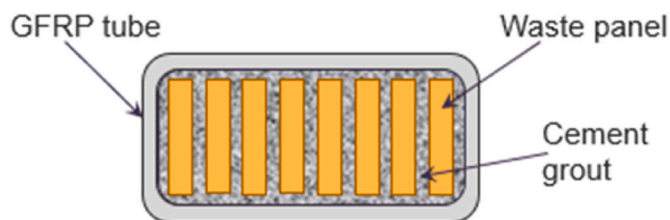


Fig. 1. Concept of composite railway sleepers.

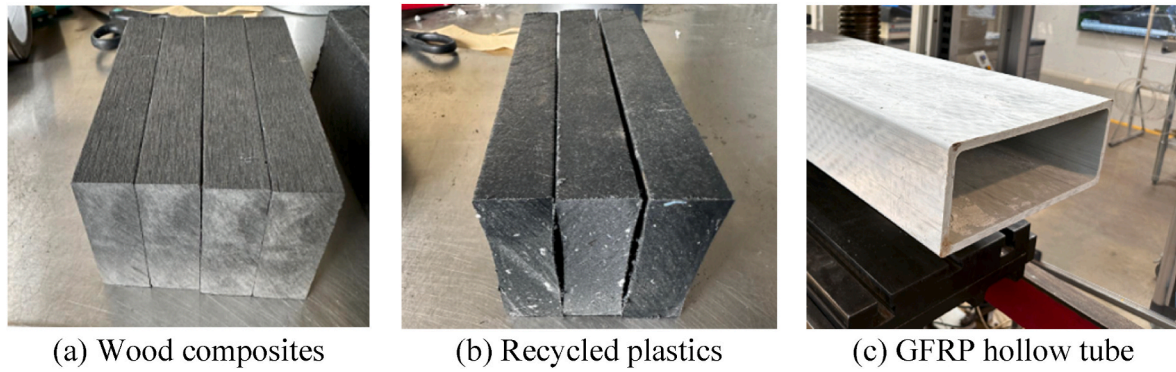


Fig. 2. Materials used in specimen preparation.

Table 1
Properties of fibre composite tube.

Properties	Fibre composite tube
Density (kg/m ³)	2030
Tensile strength (MPa)	610
Tensile modulus (GPa)	36
Poisson's ratio	0.28
Compressive strength (MPa)	485
Compressive modulus (GPa)	33
In-plane shear strength (MPa)	84
In-plane shear modulus (GPa)	4.28

Table 2
Design Parameters and Levels of selected parameters.

Design Parameters, P _d	Levels		
	1	2	3
A Water/cement ratio	0.35	0.4	0.45
B Bond thickness, T	3	5	10
C Panel types	Wood	Plastic	Combination
D Surface coating	Plain	Sanding	Sand coating

Table 3
L₉(3⁴) Designing experiments with orthogonal arrays.

Expt. No.	w/c ratio	Bond thickness, mm	Panel types	Surface coating
E-1	0.35	3	Wood	Plain
E-2	0.35	5	Plastic	Sanding
E-3	0.35	10	Combination	Sand coating
E-4	0.4	3	Plastic	Sand coating
E-5	0.4	5	Combination	Plain
E-6	0.4	10	Wood	Sanding
E-7	0.45	3	Combination	Sanding
E-8	0.45	5	Wood	Sand coating
E-9	0.45	10	Plastic	Plain

freedom each, making the total degree of freedom (DOF) eight in this study. Consequently, Taguchi L₉(3⁴) arrays could be used, which offer the same degree of freedom. Conversely, Eq (2) provides a method for determining the minimum number of experiments (N) required based on the design parameters (Pd) and level (L).

$$N = 1 + (L - 1)P_d \quad (2)$$

2.2.2. Signal-to-noise ratio (SNR) and analysis of variance (ANOVA)

The deviation between the experimental and desired values is determined by using a loss function to determine the influence of design parameters. In the Taguchi method, the loss function is further transformed into the SNR, which represents the expected outcome in a logarithmic manner. Taguchi's method relies on three different models

[23] of the SNR to achieve the following objectives: (a) nominally the best - achieve the highest response with the least deviation; (b) larger the better - achieve the highest response; and (c) smaller the better - achieve the lowest response. Eqs. (3)–(5) can be used to express each of these models.

$$\text{Nominal the best, } SNR = 10 \log \left(\frac{\bar{y}_i^2}{\sigma_i^2} \right) \quad (3)$$

$$\text{Larger the better, } SNR = -10 \log \left(\frac{1}{n} \sum_{j=1}^n \frac{1}{y_j^2} \right) \quad (4)$$

$$\text{Smaller the better, } SNR = -10 \log \left(\frac{1}{n} \sum_{j=1}^n y_j^2 \right) \quad (5)$$

where,

$$\bar{y}_i = \frac{1}{n} \sum_{j=1}^n y_{ij} \quad (6)$$

$$\sigma_i^2 = \frac{1}{n-1} \sum_{j=1}^n (y_{ij} - \bar{y}_i)^2 \quad (7)$$

In Eqs. (6) and (7), *n* denotes the number of trials, *i* is the number of experiments, *j* the number of trials, \bar{y}_i the mean value of the observed data, and σ_i^2 the variance of the observed data.

While the SNR analysis can rank the design parameters according to their influence on the final output, it cannot quantify the extent to which each parameter has an effect. This can be accomplished using ANOVA, a statistical technique used for interpreting experimental data and making decisions. The total variability can be separated from the SNR in order to determine the relative contribution of each parameter. In most cases, the relative significance of an effect is determined by the F value, which is a ratio between the mean of squared deviations and the mean of squared errors, where a higher value indicates a larger effect. As a result of overfitted designs, residual sums of squares have zero degrees of freedom; therefore, the percentage contribution of each parameter can be determined directly using equations (8)–(10).

$$\text{Contribution percentages of each parameter} = \frac{SS_k}{SS_T} \times 100 \quad (8)$$

where *SS_T* the total sum of squares of all parameters and *SS_k* denotes the sum of squares for the *k* th parameter.

$$SS_k = \sum_{j=1}^L n \left[(SNR)_{kj} - SNR_T \right]^2 \quad (9)$$

where *n* is the number of trials for each experiment at level *j* of parameter *k*, *SNR_T* the overall mean of the SNR, *L* is the level numbers

and N is the number of total experiments.

$$SS_T = \sum_{i=1}^N [(SNR)_i - SNR_T]^2 \quad (10)$$

2.3. Specimen preparation and test setup

2.3.1. Bond specimen preparation and testing

The use of a double-leg specimen configuration was designed to examine the effects of the design parameters on the bond behaviour (Fig. 3). It is necessary to understand the bond behaviour of composite wood and recycled plastic panels before performing the full-scale composite beams. In this study, nine different specimens were prepared using Taguchi’s design of experiment (3 replicates per specimen). Composite wood panels measuring 75 mm wide by 25 mm thick and recycled plastic panels measuring 70 mm wide by 20 mm thick were cut to 150 mm lengths. The middle panel was 25 mm larger than the side panels to facilitate load application. The composite panels (wood composites and recycled plastics) were attached with cement grouts of various thicknesses (3 mm, 5 mm and 10 mm) and surface conditions (plain, sanding and sand coating). Loads were applied in compression mode on the extended portion of the middle panel, which resulted in the specimens failing in shear mode. An investigation of the bond between composite wood and plastic panels was conducted, and the results revealed how composite panels will behave inside GFRP tubes if composite beams are manufactured.

2.3.2. Manufacturing of composite beams and testing

GFRP pultruded rectangular hollow sections were filled with composite wood and recycled plastic panels, which were bonded together with cement grout to manufacture the composite beams. The beam concepts are illustrated in Fig. 4. The rectangular hollow section (RHS) of GFRP considered was 1.60 m long, 250 mm wide, and 100 mm deep, with a wall thickness of 8.1 mm. Inside hollow GFRP profiles, composite wood and plastic profiles were placed flatwise (horizontally) and edgewise (vertically), and the results were compared with hollow profiles. The gap was filled with cementitious grout, which binds the panels

together.

Four beams were tested (Fig. 4) in this study: (a) a hollow GFRP profile, (b) a GFRP profile filled with recycled plastic panels in edgewise orientation, (c) a GFRP profile filled with recycled plastic panels in flatwise orientation, and (d) a GFRP profile filled with composite wood in edgewise orientation. The hollow sections were used to study the effect of filling, but they were not considered sleeper concepts since they were unable to support screws for rail fastenings and collapsed under train wheel loads.

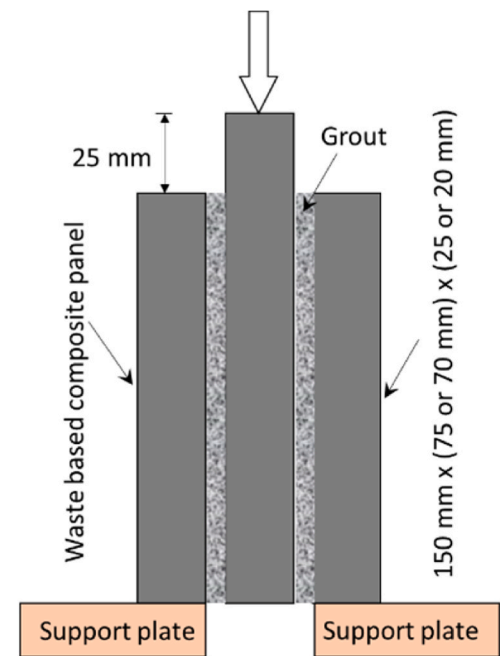
The beams were tested using the 400 kN capacity testing equipment under different span lengths (L), including 400 mm, 800 mm, and 1200 mm. To understand the effects of the span-to-depth ratios of the beam, non-destructive tests were conducted at spans of 400 mm and 800 mm. The beam was destructively tested to determine its ultimate load-bearing capacity under three-point bending over a span of 1200 mm. Two strain gauges were attached at the midspan of each beam to investigate compression and tensile strain behaviour. The top strain gauge was slightly off-centre of the beam to provide sufficient space for the loading plate. The bottom strain gauge was attached at the centre of the beam where there was the greatest deflection. Testing was conducted carefully to ensure that the strain gauges would not be damaged during the movement of the beam for testing at different span lengths. A stress and strain diagram were plotted accordingly. The failure characteristics of the beam were examined and identified during the tests.

3. Results and discussion

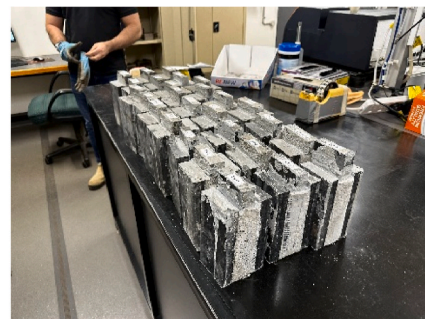
3.1. Bond behaviour of panels

3.1.1. Bond failure behaviour of panels

Testing was conducted under compression loading to determine bond failure behaviour. In this test method, the load is evenly distributed across two separate legs so that the bonded interface is subjected to a shearing force parallel to the adhesion plane. The force needed to separate the adherends provides valuable insight into the effectiveness of the bonding agent and the quality of surface preparation. It is important to note that a high shear bond strength indicates that there is a



(a) Schematic diagram of bond test



(b) Bond specimens and testing

Fig. 3. Bond behaviour investigation of Waste-based Panels.

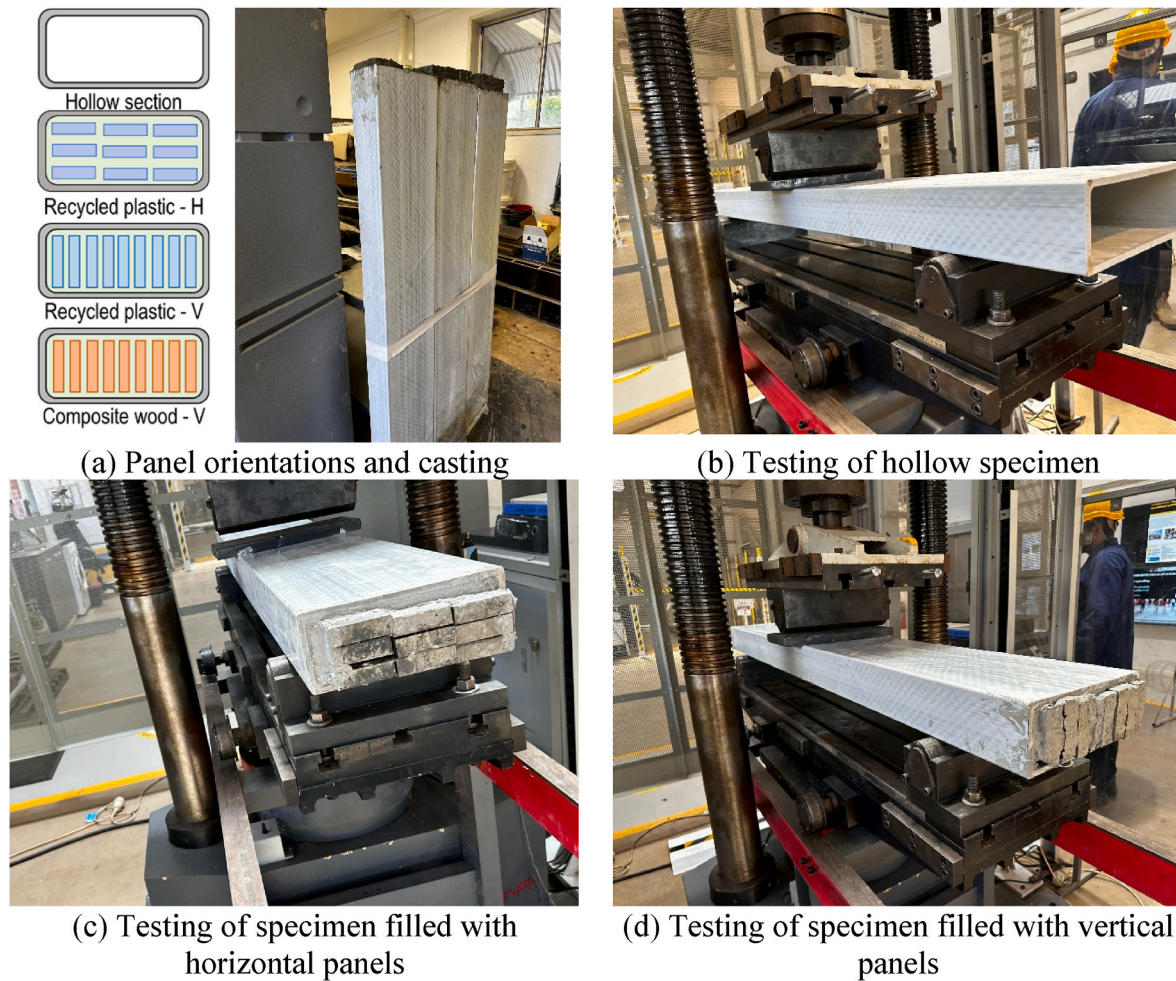


Fig. 4. Casting and testing of specimens.

robust adhesion and cohesive integrity in the bond, which ensures structural stability. Visual inspection of the samples was conducted, and failure behaviour was noted. Surface conditions and bond thickness both contributed to failures of both cohesive and adhesive bonds. Rough surfaces demonstrate more strength than smooth surfaces when it comes to bonding. Plastic material, for example, exhibits adhesive failure because of their relatively smooth surfaces. On the other hand, wood

panels have a rough surface, and the failure pattern is cohesive, as illustrated in Fig. 5.

During compression loading, the specimens experienced shear stress in the joint area, as measured by Eq. (11) and presented in Fig. 5(c). It is evident that the bond strength varies between specimens. This is due to the variation in the design parameters. A large variation in bond strength from one sample to another indicates that the selected design

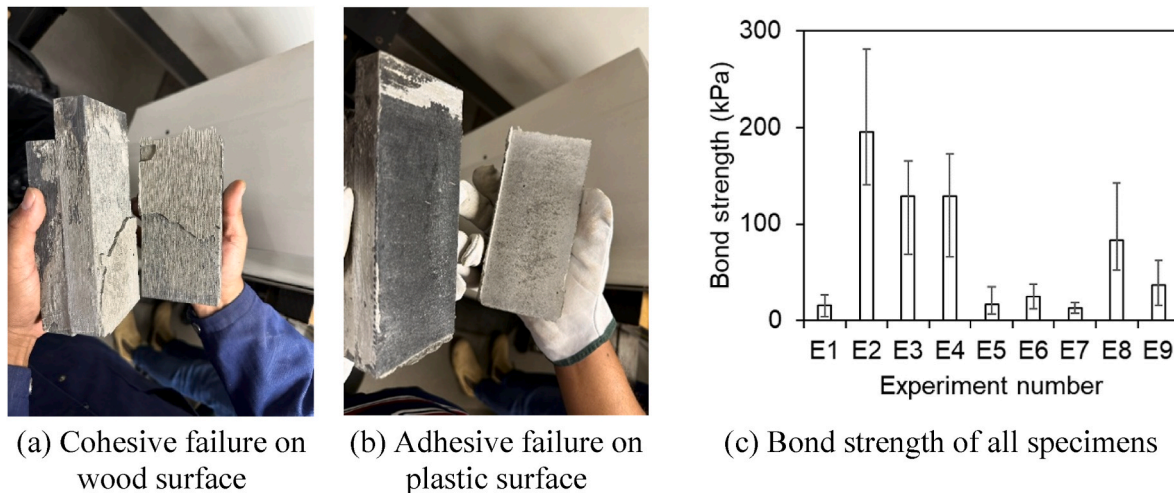


Fig. 5. Failure and strength behaviour of wood composite and recycled plastic panels.

parameters have a significant impact on bond strength. Furthermore, replicate specimens within the same group of samples showed a high degree of variation. Perhaps this is due to the complex nature of the bond specimen's shear behaviour, which has also been observed in previous studies [20].

$$\text{Shear bond strength} = \frac{\text{Failure load}}{2(\text{Bond length} \times \text{Bond width})} \quad (11)$$

3.1.2. Analysis of experimental variables

The mean of signal to noise ratio (SNR) was plotted against the different parameters that affected bond strengths, including water-cement ratio, bond thickness, panel type, and surface coating (Fig. 6). The results from nine experiments, including failure loads, strengths, standard deviations, signal-to-noise ratios (SNRs), and the overall average of SNRs, are investigated. In light of the fact that the purpose of this study was to know the bond strength between composite panels and cement grout, it follows that the quality characteristic specified in Eq. (4) is a "larger-the-better" criterion, indicating greater bond strength.

3.1.3. Effect of water-cement ratio on bond strength

The effect of the water-cement ratio on bond strength is shown in Fig. 6 (a) in relation to the mean SNR. In general, the SNR value decreases as the water-cement ratio increases. In the case of a water-cement ratio of 0.35, the SNR value was 34, while it decreased to approximately 28 in the case of a water-cement ratio of 0.40 and 0.45. Cement grout strength can have a significant impact on bond strength. It is well known that grout strength deteriorates with an increase in the water-to-cement ratio. Furthermore, excess water in the grout can increase porosity, decrease density, and make it more susceptible to cracking and degradation. In the presence of voids, the effective bond surface is reduced, resulting in bond failure at lower loads. Therefore, a water-to-cement ratio of 0.35 was selected for the manufacturing of composite beams.

3.1.4. Effect of bond thickness on bond strength

Fig. 6(b) illustrates the relationship between bond thickness and bond strength as expressed by the mean signal-to-noise ratio (SNR). For a bond thickness of 3 mm, the SNR was 26.09, whereas it increased to 33.34 for a bond thickness of 5 mm, and then decreased to 30.96 for a bond thickness of 10 mm. Strength and integrity of bonded materials are determined by the thickness of the bond layer. Excessively thick bond layers (e.g., 10 mm) may result in stress concentrations and reduced performance. On the other hand, thin bond layers may exhibit a lower bond strength due to their proneness to failure under load. The findings are also consistent with the effect of polymer bond thickness on sandwich panels in a previous study [20]. The proper thickness of a bonded assembly is therefore essential for maximising bond strength and ensuring its long-term performance and durability. The study determined that a 5 mm thick bond is more appropriate than others.

3.1.5. Effect of panel types on bond strength

The impact of panel types on bond strength displaying the average signal-to-noise ratio (SNR) is illustrated in Fig. 6(c). The composite panel types were chosen wood, plastic and a combination of wood and plastic. The plastic panel shows a greater SNR value (37.46) comparing to wood panels (26.14) and combination of plastic-wood panels (26.80). The variation of bond strength is due to the different types of failure for different panels. The bond on the wood surface fails cohesively while the bond on the plastic surface fails adhesively. This is because the surfaces of the plastic panels were smoother than those of the wooden panels. This can be attributed to the fact that wood composites and recycled plastic panels are derived from different ingredients (60 % wood powder with 30 % HDPE and 10 % additives for wood composites, and 100 % recycled HDPE and PP for recycled plastic panels) and are manufactured (pressure-temperature extrusion for wood composites, and injection moulding for recycled plastic panels) differently. It is interesting to note that the SNR values for wood and combination samples are similar. This occurred because of the cohesive failure of wood panels in both cases. In

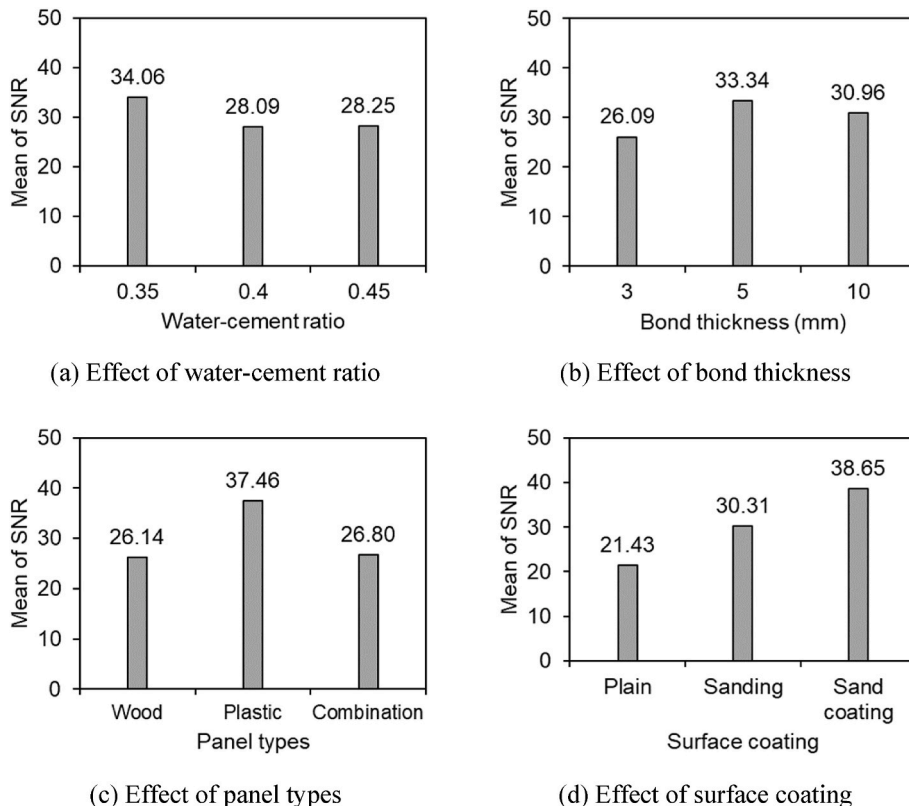


Fig. 6. Effect of different design parameters on bond strength.

this regard, it can be concluded that the combination of different panels does not necessarily improve the bond properties.

3.1.6. Effect of surface coating on bond strength

Treatment of smooth surfaces by sand coating and sanding has a significant effect on bond strength which has shown Fig. 6(d). Plain surfaces without treatment also investigated along with experiment to know the difference between with or without surface treatment. Among all these samples, the specimens with sand coating (38.65) have a greater SNR value comparing sanding (30.31) and plain surfaces (21.43). There is a reasonable expectation that surface roughness will affect the bonding behaviour. The level of surface treatment depends on the application and the cost of construction, which must be taken into consideration during the design process. The interesting finding is that the bond strength can be increased almost twice with an inexpensive method of sand coating in comparison with plane surfaces.

3.1.7. Contributions of design parameters to bond strength

Although the SNR analysis provides a ranking of design parameters based on their influence on bond strength, it does not offer insight into the specific contribution of each parameter to the development of bond strength. This contribution can be determined through ANOVA, which investigates the extent to which each parameter contributes to bond strength by partitioning the total variability of the SNR. The sum of squares for each design parameter (SS_k) and the total sum of squares for all parameters (SS_T) are calculated using Eq. (9) and Eq. (10) respectively, and then the percentage contribution of each parameter is determined using Eq. (8), as provided in Table 4.

In Tables 4 and it can be seen that surface coatings make the greatest contribution to bond strength development, accounting for 53 % of the development. The properties of the panel types and the bond thickness are the next two influential parameters, each contributing 29 % and 10 %. In contrast, the water-to-cement ratio has the least impact on bond strength development, contributing only 8 %. This is due to the contribution of sand coating to increasing surface roughness, whereas the other methods do not contribute to the increase in roughness. According to these results, the surface coating and panel type are the two most critical parameters for designing a cement grout-bonded structure.

3.2. Flexural behaviour of beams

3.2.1. Failure mode of beams

Different kinds of damages were noticed with the increase in displacement of GFRP profiles under loading, which varied depending on the types of infilled materials. The subsequent section elaborates on the failure patterns of GFRP profiles observed in laboratory experiments, as depicted in Fig. 7.

- Bending failure: A tensile rupture occurred on the bottom surface of the GFRP beam, followed by damage to the top surface of GFRP profile (Fig. 7(b)) and internal panels of the composite beam. Despite the tensile strength (610 MPa) of the GFRP profile being greater than its compressive strength (485 MPa), the tensile failure occurred before the compressive failure due to the loading plate located in the

compression zone, which distributed stresses over a wider area. A loud noise just prior to ultimate failure confirmed that the internal panels had been damaged. The ultimate failure of the exterior GFRP profile occurred immediately following the tensile bending failure at the bottom. The bending failure was observed in hollow beams and in beams with vertically filled panels.

- Shear failure: A horizontal shear crack was observed on the vertical faces of the GFRP profile when it was filled with horizontal panels (Fig. 7(c)). This type of failure occurs when the beam fails horizontally rather than by bending due to a shear stress exceeding the material's shear strength.
- Exterior GFRP compression and fibre buckling: The GFRP profiles were damaged due to the compression at the top. This type of damage occurred in both hollow and filled profiles with vertical panels. The excessive deformation of beams, however, results in skin separation and buckling on the top surface of the beams (Fig. 7(d)).

3.2.2. Load-strain behaviour of beams

Load versus strain plots have been generated for the four specimens illustrated in Fig. 8. The linear load-displacement behaviour was observed across all spans, including 400 mm, 800 mm, and 1200 mm indicating the structural behaviour was mostly dominated by exterior GFRP tube. Spans were selected based on the shear span-to-depth ratio (i.e., a/d) which determines how the beams behave. Among the test specimens, the a/d ratio was 2, 4, and 6, which indicates a wide range of characteristics ranging from shear to bending. The failure strain of the beam specimens was found to be lower than the ultimate strain of the GFRP material (0.015). These results indicate that the beam specimens did not fail as a result of pure bending. The failure was caused by a combination of bending, shear, and damage to the infilled panels.

3.2.3. Effect of filling hollow tubes

The effect of filling hollow tubes was studied by comparing the behaviour of hollow tube with tube that has been filled (Fig. 9). Filling hollow tubes increases the beam's strength and stiffness. It was observed that the strength of the beam increased by 2.3 times and the stiffness increased by 25 % when the hollow tube was filled with recycled plastic panels, as shown in Fig. 9(b). Infill panels contribute more to strength than stiffness by preventing premature failure of the beam. Performance was improved due to the increase in internal resistance to bending and the enhancement of overall structural integrity, which prevented premature local failure of the beam. It was found that the failure strength and strain of the filler (i.e., recycled plastic material) were 27 MPa and 0.035, respectively, which indicates that the confinement effect created by the external GFRP tube was highly influential on the overall structural performance. A filled tube demonstrated a slight nonlinear behaviour in the compression side of the beam just prior to failure, while a hollow tube failed suddenly at the peak load. In real-life applications, this nonlinearity of the filled tube could be interpreted as a warning of the ultimate failure of the beam.

3.2.4. Effect of infill panel orientations

The effect of infill panel orientations, flatwise (i.e., horizontal) and edgewise (i.e., vertical) orientations within the GFRP tubes were

Table 4 Percentage contribution of each parameter.

Parameter	DOF		Sum of squares		F-Value	% Contribution $(\frac{SS_k}{SS_T} \times 100)$
	$L - 1$	$N - 1$	SS_k	SS_T		
Water/cement ratio	2	8	70	839	-	8
Bond thickness	2		82		-	10
Panel types	2		242		-	29
Surface coating	2		445		-	53
Error	-		-		-	-

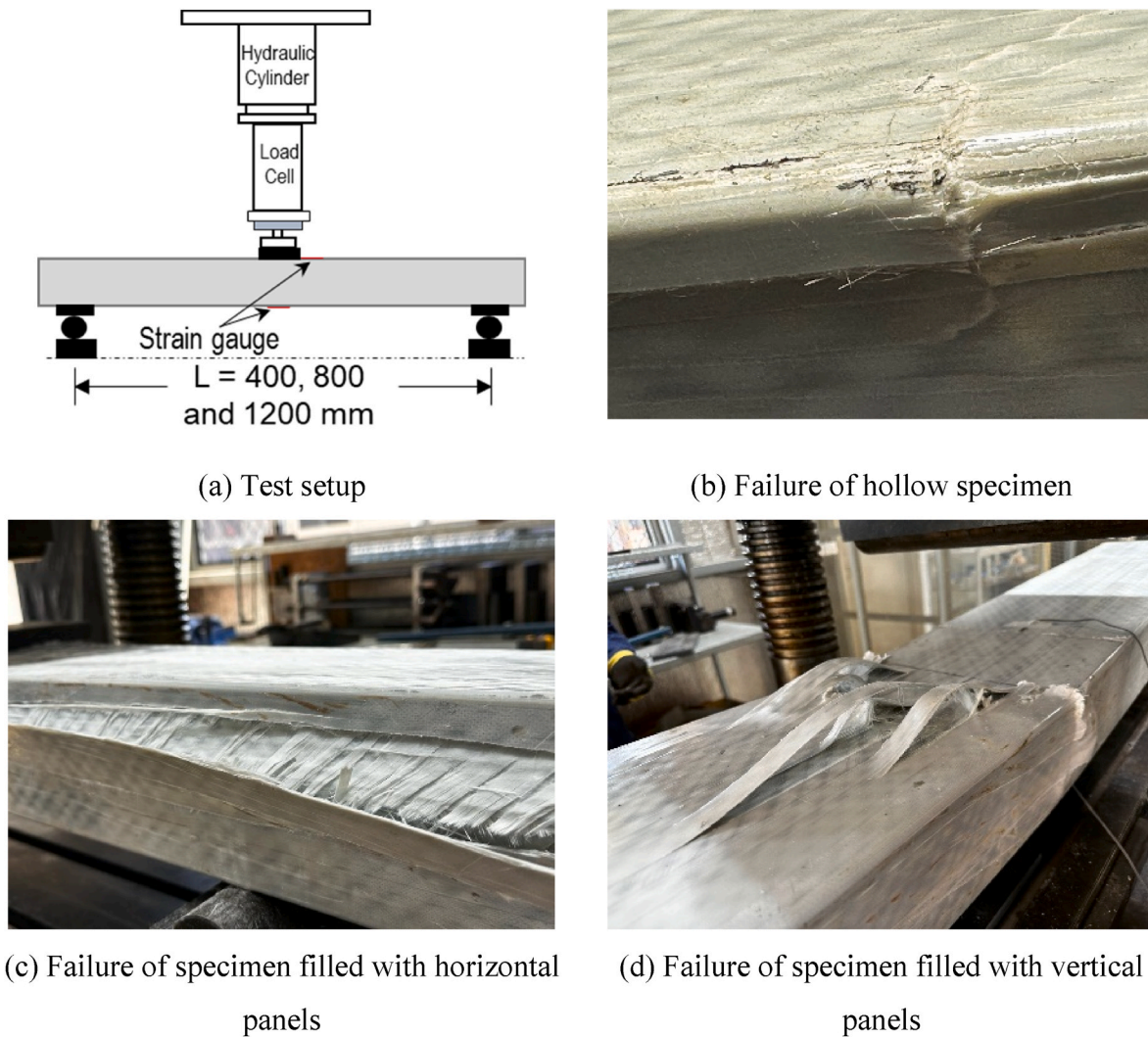


Fig. 7. Failure of beam specimens for different orientations of panels.

compared (Fig. 10). The GFRP profiles filled with recycled plastic panels with horizontal orientation (RP-H) and vertical orientation (RP-V) behave almost identically in terms of strength (163 MPa and 156 MPa) and stiffness (26.8 GPa and 26.4 GPa). This can be explained by the volume of infill materials and the properties of those materials. The internal panels were oriented horizontally as well as vertically, occupying the same volume space, and their properties did not affect the beam behaviour due to their homogeneous material properties. The slight variation can be attributed to the higher deflected capacity of horizontal panels when compared to vertical panels, which can be observed in the compression side of the stress-strain graph prior to failure (Fig. 10(a)). The horizontal panel shows a 50 % drop of load, while the vertical panel shows an 80 % drop at ultimate failure. Perhaps the horizontal panels failed due to horizontal shear failure of the cement grout, whereas the vertical panels failed due to bending cracks. This statement is also in agreement with the previous investigation where layered sandwich panels failed by bending cracks in the vertical direction, and horizontal panels failed by horizontal shear cracks [24].

3.2.5. Effect of infill panel material types

The effects of infill panel materials were studied by comparing the behaviour of recycled plastic filled GFRP tubes with composite wood filled GFRP tubes (Fig. 11). The composite wood and plastic panels were placed vertically in the GFRP profile to determine the strength and stiffness of the beam. While infill panel types with composite wood and

plastic panels resulted in similar strength (156 MPa vs 161 MPa), stiffness behaviour differed (26.4 GPa vs 29.3 GPa). It is believed that this is due to the characteristics of the infill material. In terms of bending strength, recycled plastic and composite wood were 27 MPa and 28 MPa, respectively, while bending modulus was 1 GPa and 2.75 GPa. This explains why both beams have a similar strength, but a slight difference in stiffness. It is interesting to note that while infilled wood composites exhibit 2.75 times greater stiffness than recycled plastics, this does not translate into a difference in beam performance. This is primarily due to the lower stiffness of the infill panels compared to the GFRP profiles (36 GPa) as well as confinement effect.

Based on the results of this study, the performance of the high-volume waste filled GFRP tubes can provide strength and stiffness of at least 156 MPa and 26.4 GPa, respectively. In comparison, this performance is superior to the strength and stiffness characteristics of timber railway sleepers, which are respectively 50 MPa and 7 GPa [6]. It is therefore evident from the initial findings of the study that it may be possible to replicate the behaviour of timber railway sleepers. It is, however, necessary to conduct a detailed investigation to determine how the beam will perform under screw pull-out and dynamic loading conditions, as these factors are extremely important when it comes to railway sleepers.

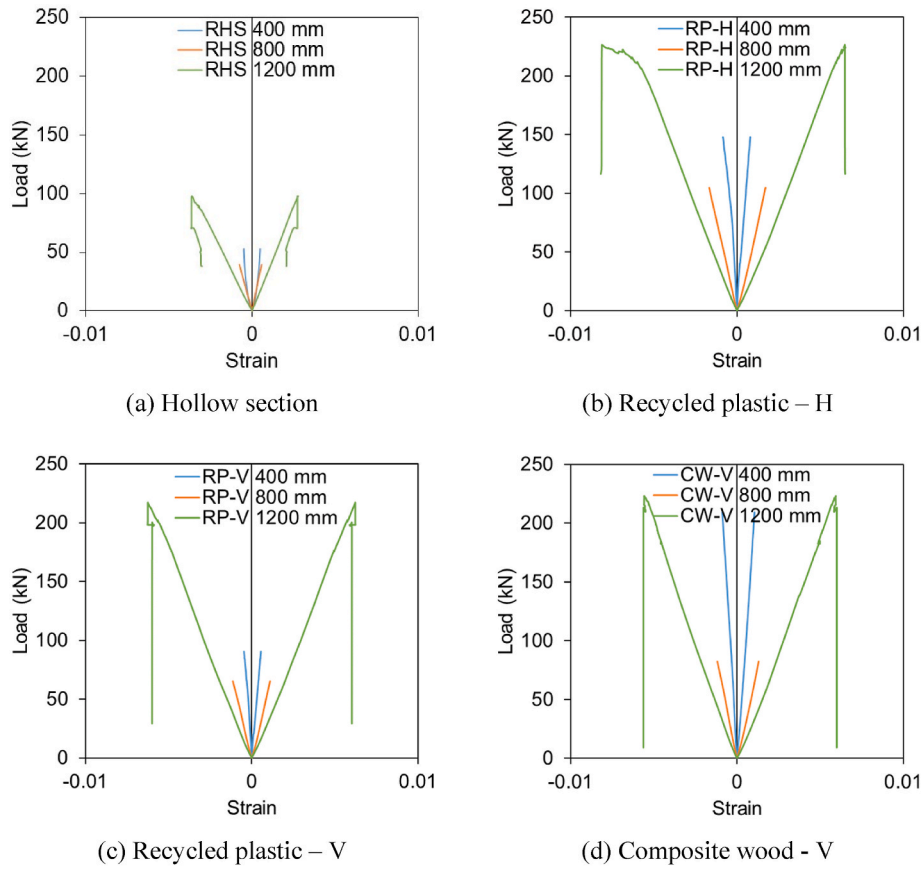


Fig. 8. Load-strain behaviour of different composite beams.

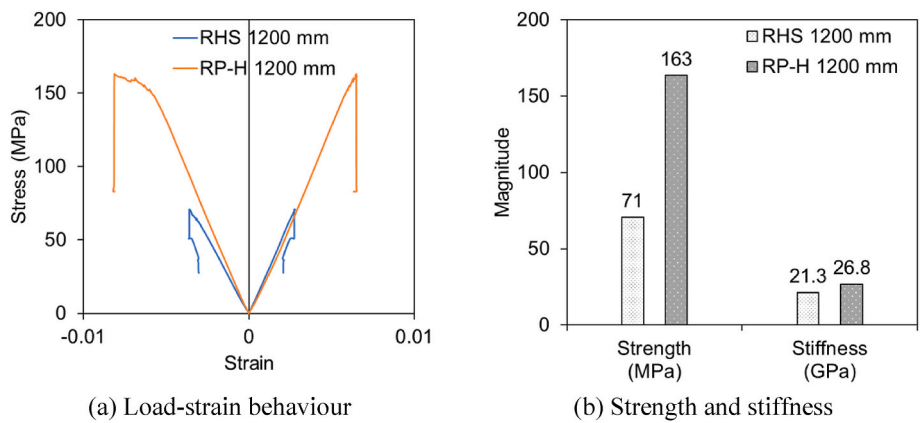


Fig. 9. Effect of filling hollow tubes.

4. Conclusions

This study investigated the bonding properties of composite wood and recycled plastic materials with cement grout and utilised them as an infill material of GFRP tubes to manufacture a composite railway sleeper. The effect of cement grout properties (water-to-cement ratio), bond thickness, panel type, and surface coating were examined to understand the bond behaviour. Moreover, the effect of filling hollow tubes, the orientation of the infill panels, and the material types of the infill panels were studied to determine whether composite beams are suitable for use as railway sleepers. The following conclusions are drawn from this study.

- Wood composites and recycled plastic panels can be bonded using simple cement grout when used as infill materials, eliminating the need for expensive resin systems for many traditional structures. The bond thickness is a significant factor in determining how the bond will fail. An excessively thick bond layer (e.g., 10 mm) may result in stress concentrations and decreased bond performance. Conversely, thin cement grout bond layers (e.g., 3 mm) have a lower bond strength due to their tendency to fail under load. A bond thickness of 5 mm is found to be most suitable.
- Wood surface bonds fail cohesively, whereas the plastic surface bonds fail adhesively, due to the smoother surfaces of the plastic panels compared to the wood surfaces. An interesting finding is that the bond strength can be increased almost twice with an inexpensive

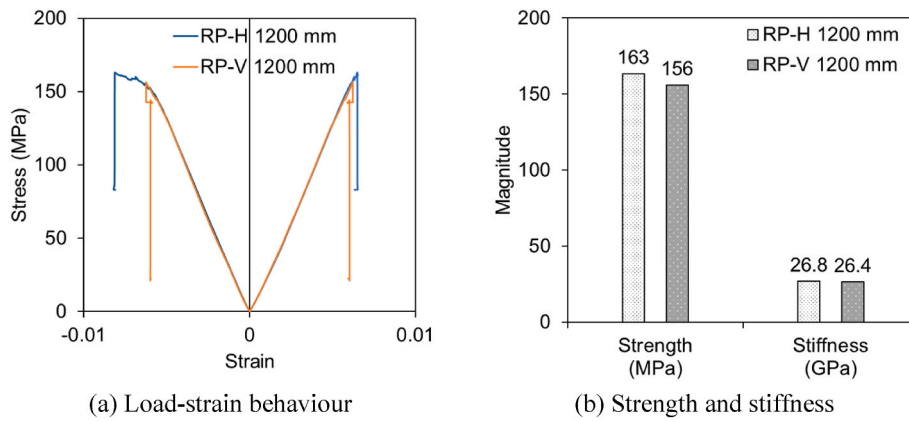


Fig. 10. Effect of in-fill panel orientations.

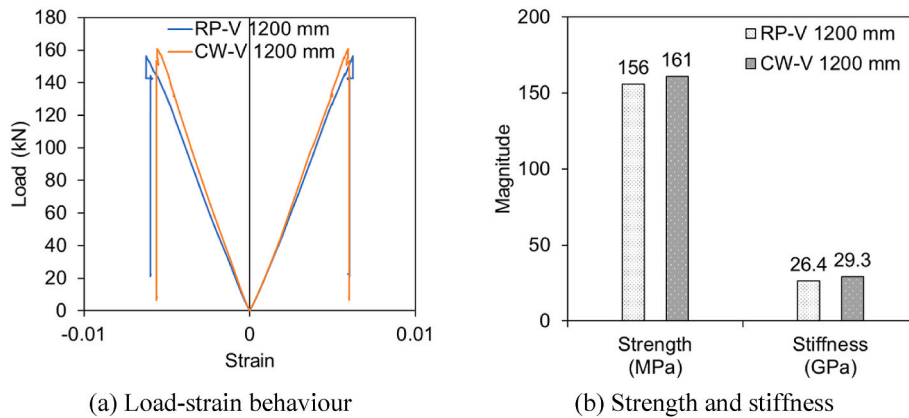


Fig. 11. Effect of in-fill panel material types.

method of sand coating in comparison with plane surfaces. In terms of improving bond strength, the surface coating is the most influential parameter, followed by the type of panel, the bond thickness, and the grout properties.

- When a hollow tube is filled with waste-based material, the strength of the tube increases significantly, while the stiffness properties are not greatly affected. Local buckling is prevented by infill materials, which enhances the structural strength of the beam. If the stiffness of the outer profile is greater than the stiffness of the infill materials, then the overall stiffness of the beam with or without infill materials is not different, since the stiffness characteristics of the beam are largely determined by the stiffness characteristics of the outer profile.
- Orientation of the infill panels flatwise or edgewise does not affect the strength or stiffness properties of the beam, provided that the infill volume remains the same and the infill material is homogenous. However, flatwise orientation of the infill panels may result in a greater residual capacity of the beam after ultimate failure than edgewise orientation.

A summary of the major conclusions from this study is that cement grout can be considered as a suitable adhesive for bonding panels together. It is possible to significantly increase bond strength by treating the bond surface, and infill panels can prevent premature tube failure, but their orientations and properties do not significantly affect the beam's behaviour. The purpose of this study was to investigate the feasibility of manufacturing composite railway sleepers using GFRP tubes filled with high volumes of waste materials. Findings indicate that the proposed concept has a high potential for replacing traditional

timber railway sleepers. It is recommended that a detail investigation on the environmental impact assessment of the proposed sleeper concept should be conducted to understand the environmental sustainability.

CRediT authorship contribution statement

Mamun Abdullah: Writing – original draft, Validation, Methodology, Formal analysis, Conceptualization. **Wahid Ferdous:** Writing – review & editing, Supervision, Methodology, Investigation, Conceptualization. **Sourish Banerjee:** Writing – review & editing, Supervision. **Ali Mohammed:** Writing – review & editing. **Allan Manalo:** Writing – review & editing, Supervision.

Declaration of competing interest

The authors declare that they have no known competing financial interests or personal relationships that could have appeared to influence the work reported in this paper.

Data availability

Data will be made available on request.

Acknowledgements

The authors would like to acknowledge Wagners Pty Ltd for their generous in-kind contributions to supply GFRP tubes. The second author would like to acknowledge the financial support he received from the Advance Queensland Industry Research Fellowship (AQIRF 098-

2021RD4) program.

References

- [1] W. Ferdous, A. Manalo, Failures of mainline railway sleepers and suggested remedies – review of current practice, *Eng. Fail. Anal.* 44 (2014) 17–35.
- [2] A. Manalo, T. Aravinthan, W. Karunasena, A. Ticoalu, A review of alternative materials for replacing existing timber sleepers, *Compos. Struct.* 92 (3) (2010) 603–611.
- [3] C.E. Bakis, et al., Fiber-reinforced polymer composites for construction — state-of-the-art review, *J. Compos. Construct.* 6 (2) (2002) 73–87.
- [4] S.M. Harle, Durability and long-term performance of fiber reinforced polymer (FRP) composites: a review, in: *Structures*, vol. 60, Elsevier, 2024 105881.
- [5] L.C. Bank, *Composites for Construction : Structural Design with FRP Materials*, John Wiley & Sons, Inc, New Jersey, 2006.
- [6] W. Ferdous, A. Manalo, G. Van Erp, T. Aravinthan, S. Kaewunruen, A. Remennikov, Composite railway sleepers—Recent developments, challenges and future prospects, *Compos. Struct.* 134 (2015) 158–168.
- [7] W. Ferdous, A. Manalo, G. Van Erp, T. Aravinthan, K. Ghabraie, Evaluation of an innovative composite railway sleeper for a narrow-gauge track under static load, *J. Compos. Construct.* 22 (2) (2018) 1–13.
- [8] W. Ferdous, et al., Static behaviour of glass fibre reinforced novel composite sleepers for mainline railway track, *Eng. Struct.* 229 (2021) 111627.
- [9] W. Ferdous, et al., Behaviour of polymer filled composites for novel polymer railway sleepers, *Polymers* 13 (8) (2021) 1324.
- [10] G. Koller, FFR synthetic sleeper – projects in Europe, *Construct. Build. Mater.* 92 (2015) 43–50.
- [11] G. Van Erp, M. McKay, Recent Australian developments in fibre composite railway sleepers, *Electron. J. Struct. Eng.* 13 (1) (2013) 62–66.
- [12] P. Sengsri, C. Ngamkhanong, A.L. O.d. Melo, M. Papaalias, S. Kaewunruen, Damage detection in fiber-reinforced foamed urethane composite railway bearers using acoustic emissions, *Infrastructures* 5 (6) (2020).
- [13] M.H. Esmaili, H. Norouzi, F. Niazi, Evaluation of mechanical and performance characteristics of a new composite railway sleeper made from recycled plastics, mineral fillers and industrial wastes, *Compos. B Eng.* 254 (2023) 110581.
- [14] AuManufacturing. Australian first: railway sleepers made of recycled plastic get type approval by Victorian operators, 2021. *Aust. Now.:* aumanufacturing.com.au 20 May.
- [15] A. Bednarczyk, New composite sleeper set to undergo live trials, *Int. Railw. J.* 28 (Feb) (2019).
- [16] COEN, COEN composite wood - building a better environment, Australia, www.coen.com.au, 2024.
- [17] Replas, Turning problem plastic, into useful products, Australia, www.replas.com.au, 2024.
- [18] Wagners, Composite Fibre Technologies - Product Guide, vol. 5, Wagners CFT Manufacturing Pty Ltd, 2021.
- [19] G. Taguchi, Y. Yokoyama, *Taguchi Methods: Design of Experiments*, ASI Press, USA, 1993.
- [20] W. Ferdous, A. Manalo, T. Aravinthan, Bond behaviour of composite sandwich panel and epoxy polymer matrix: Taguchi design of experiments and theoretical predictions, *Construct. Build. Mater.* 145 (2017) 76–87.
- [21] A. Hosseini, D. Mostofinejad, Effective bond length of FRP-to-concrete adhesively-bonded joints: experimental evaluation of existing models, *Int. J. Adhesion Adhes.* 48 (2014) 150–158.
- [22] M. Abdullah, W. Ferdous, S. Banerjee, A. Manalo, Bond behaviour of smooth surface GFRP pultruded profiles with cement grout, *Case Stud. Constr. Mater.* 20 (2024) e02891.
- [23] R.S. Kumar, K. Sureshkumar, R. Velraj, Optimization of biodiesel production from Manilkara zapota (L.) seed oil using Taguchi method, *Fuel* 140 (2015) 90–96.
- [24] W. Ferdous, A. Manalo, T. Aravinthan, A. Fam, Flexural and shear behaviour of layered sandwich beams, *Construct. Build. Mater.* 173 (2018) 429–442.